Inverse Temperature Dependent Lifetimes of Transient S_N2 Ion-Dipole Complexes

J. Mikosch, R. Otto, S. Trippel, C. Eichhorn, M. Weidemüller, and R. Wester*

Physikalisches Institut, Universität Freiburg, Hermann-Herder-Strasse 3, 79104 Freiburg, Germany

Received: May 27, 2008; Revised Manuscript Received: August 8, 2008

The association and collisional stabilization of the S_N2 entrance channel complex $[Cl^-\cdots CH_3Cl]^*$ is studied in a low-temperature radiofrequency ion trap. The temperature dependence of the ternary rate coefficient is measured and a much stronger inverse temperature dependence than expected from a simple statistical calculation is found. From these data the lifetime of the transient S_N2 complex has been derived as a function of temperature. It is suggested that the inverse temperature dependent rates of nonsymmetric S_N2 reactions are related to the observed inverse temperature dependence of the transient ion-dipole complexes.

1. Introduction

Many chemical reactions proceed via one or more transient intermediate complexes, and the lifetime of these complexes is decisive for the outcome of the reaction. Gas phase nucleophilic substitution (S_N2) reactions,[1−7] textbook examples for chemical reactions, represent important model systems to investigate complex lifetimes and their effects in detail.[1,8−11] In the course of a typical S_N2 reaction

$$X^- + CH_3Y \rightarrow XCH_3 + Y^- \qquad (1)$$

two transient ion-dipole collision complexes $[X^-\cdots CH_3Y]^*$ and $[XCH_3\cdots Y^-]^*$ are subsequently formed, which are separated by a Walden inversion of the CH_3 umbrella. A key factor in determining the overall rate coefficient for these reactions is the ratio of the decay rates of the entrance channel complex to products versus back to reactants. The dynamical hindrance of traversing the central barrier[12] is the reason why the rates of most S_N2 reactions are significantly lower than the capture rate.[13] This is supported by trajectory calculations of the lifetime of the entrance channel complex.[4,14,15] In addition, S_N2 reactions may proceed directly by avoiding trapping in the ion-dipole complexes, in violation of the assumptions of statistical theories.[4] Further nonstatistical behavior that is observed for S_N2 reactions is attributed to a shorter lifetime of the metastable complexes compared to the time needed for vibrational energy redistribution among the inter- and intramolecular modes. Particular examples of nonstatistical reactivity are different reaction rates for vibrational as compared to translational excitation of the reactants[16] and the preferential partitioning of the excess energy into product rotation and vibration as compared to translation.[7,17,18] Transient complexes with longer lifetimes show a better agreement with statistical calculations.[9] However, also for larger S_N2 complexes explicitly nonstatistical dynamics has been found.[19]

To understand the fragmentation dynamics of metastable S_N2 complexes, studies of the dependence of the lifetime on the excess energy of the complex are important. Classical trajectory calculations show multiexponential decay curves with a moderate increase of the average lifetime with decreasing excess energy.[15,20] In the same work it is shown that the obtained energy-dependent average lifetimes disagree strongly with statistical calculations, unless energy redistribution in the statistical model is restricted to only few vibrational modes. Reduced-dimensional quantum scattering calculations reveal many narrow Feshbach resonances with a broad range of associated lifetimes,[21−26] which are difficult to reconcile with the classical trajectory results at the current level of theory. Indirect experimental evidence for an energy dependent lifetime of an S_N2 complex comes from temperature-dependent reaction rate coefficient measurements of $Cl^- + CH_3Br$.[27] Here, a steep decrease of the rate coefficient by several orders of magnitude with increasing temperature has been observed, which is explained by an increased decay rate of the complex back to reactants due to the increased reactant density of states. To clarify this interpretation and to guide the different theoretical approaches, dedicated experiments on energy-dependent complex lifetimes are needed.

Despite the importance of obtaining lifetimes of metastable complexes, only two direct measurements of S_N2 complex lifetimes have been carried out to date.[10,11] On the one hand, a high pressure mass spectrometry study using collisional stabilization has resulted in a lifetime of 12 to 16 ps for $[Cl^-\cdots CH_3Cl]^*$ at a fixed temperature of 296 K.[10,28] On the other hand, time-resolved tracking of the dissociation of $[I^-\cdots CH_3I]^*$ has revealed a biexponential decay with dissociation lifetimes of 0.8 and 10 ps for S_N2 complexes with roughly 20 meV relative energy above the asymptote.[11]

In this work we measure lifetimes of S_N2 anion−dipole complexes in a thermalized low-temperature environment. We extract these lifetimes, similar to the work of ref 10, from ternary rate coefficients for the formation and collisional stabilization of the complexes. Using a temperature-variable radiofrequency ion trap to thermalize the Cl^- and CH_3Cl reactants in a low density environment, we obtain lifetimes as a function of the reactant temperature. In the unimolecular decay process, this temperature describes the distribution of excess energies above the energy asymptote of the reactants. For cationic reactions, the extraction of complex lifetimes from ternary association has a long history using flow and drift tubes at high pressure[29−32] and has also been performed in a radiofrequency ion trap at lower densities.[33] The interpretation of these experiments is based on statistical phase space theories,[34−37] and good agreement is usually found.[38] Here we investigate the symmetric anion-molecule S_N2 reaction

---

* To whom correspondence should be addressed. E-mail: roland.wester@physik.uni-freiburg.de.

10.1021/jp804655k CCC: $40.75

$$Cl^- + CH_3Cl \rightarrow ClCH_3 + Cl^- \qquad (2)$$

specifically the formation and the unimolecular decay time of the metastable [$Cl^- \cdots CH_3Cl$]* entrance channel complex. The potential energy as a function of the difference of the two C−Cl interatomic distances Δr(C−Cl), the reaction coordinate, is shown in Figure 1.[39] It shows the double-minimum structure characteristic to S$_N$2 reactions, where the minima correspond to ground-state entrance and exit channel ion-dipole complexes. The computed binding energy with respect to the asymptotes is about 450 meV, in reasonable agreement with experimental data from collision induced dissociation experiments and high-pressure mass spectrometry.[10,40−43] For comparison, the dashed line shows the long-range electrostatic potential calculated for the interaction of the Cl$^-$ ion with the permanent and induced dipole moment of CH$_3$Cl.

The formation and the unimolecular decay of the entrance channel complex [$Cl^- \cdots CH_3Cl$]* represent the first steps that determine how reaction (2) proceeds from reactants to products. The next step, the transition of the central barrier in the potential energy surface is strongly suppressed at thermal energies due to the height of the intermediate barrier calculated to lie more than 100 meV above the asymptotes (see Figure 1), which becomes manifest in the low rate coefficient for reaction (2).[44] The exact value of the barrier height is still under debate.[40]

2. Experimental Procedure

The ternary association experiment is carried out in a cryogenic 22-pole radiofrequency ion trap.[45−47] Such cryogenic ion traps are ideal tools for the study of chemical reactions and laser-induced processes at low temperatures.[33,46,48−53] The efficient buffer gas cooling of translational and internal degrees of freedom of molecular ions has been shown by action spectroscopy.[54−56] It is estimated from the ion-neutral collision rate to occur within hundreds of microseconds.

Three-body association in the thermal environment of the ion trap can be understood as a two-step process (see also Figure 1)

$$Cl^- + CH_3Cl \underset{k_\Gamma}{\overset{k_f n_{CH_3Cl}}{\rightleftharpoons}} [Cl^- \cdots CH_3Cl]^* \xrightarrow{k_s n'} [Cl^- \cdots CH_3Cl] \qquad (3)$$

In the first step collisions of Cl$^-$ anions with neutral CH$_3$ Cl form the ion-dipole complex [$Cl^- \cdots CH_3Cl$]*, which is highly excited with respect to its ground state. This proceeds at the rate $k_f n_{CH_3Cl}$, where k_f denotes the capture rate coefficient and n_{CH_3Cl} the methyl chloride density. The metastable complex disscociates back to reactants with the unimolecular rate k_Γ. Stabilization of the complex only occurs if a third particle impact removes more internal excitation from the complex than the initial relative translational and internal energy of its constituents. Given the deep well in the potential only a fraction of the internal excitation of the complex [$Cl^- \cdots CH_3Cl$]* needs to be removed to prevent dissociation. In further collisions thermalization of the internal energy with the buffer gas temperature occurs. Re-excitation of the thermalized complex above the dissociation asymptote is then strongly suppressed by a Boltzmann factor and is therefore not considered. The rate of stabilization is given by $k_s n'$, where k_s is the rate coefficient for inelastic collisions and n' is the density of the neutral stabilizing agent. Under the low density conditions of the experiment stabilization of the complex is a rare event; the time scale for collisions is about 10 μs as compared to expected complex lifetimes in the range of picoseconds. Hence the low-pressure limit of the steady state approximation is valid and the overall rate of product formation in reaction (3) can be written as

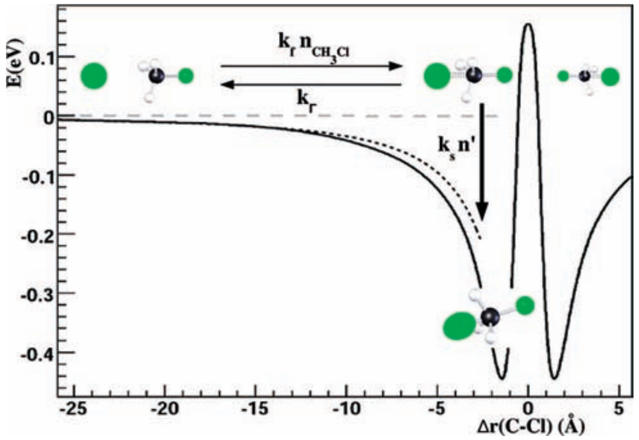

Figure 1. Potential energy of the symmetric S$_N$2 reaction $Cl^- + CH_3Cl \rightarrow ClCH_3 + Cl^-$ as a function of the reaction coordinate. The dashed line shows the long-range ion-dipole interaction potential. The arrows denote the association, fragmentation and stabilization processes of the [$Cl^- \cdots CH_3Cl$] complex and their corresponding rates.

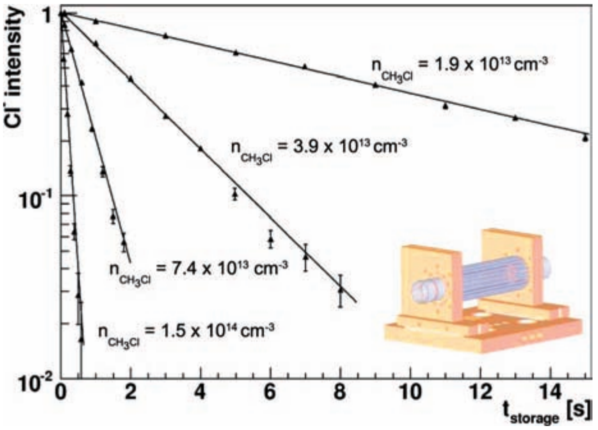

Figure 2. Decay curves of the intensity of Cl$^-$ anions in the 22-pole trap at 150 K as a function of the storage time for different densities of the CH$_3$Cl reactant molecule. The density-dependent Cl$^-$ loss rates are obtained from monoexponential fits to the data. The inset shows the temperature-variable 22-pole radiofrequency ion trap employed in the experiment.

$$R = \frac{k_f k_s}{k_\Gamma} n_{CH_3Cl} n' = k_3 n_{CH_3Cl} n' \qquad (4)$$

The three-body rate coefficient $k_3 = k_f k_s / k_\Gamma$ is determined from a measurement of the Cl$^-$ decay rate R as a function of the densities n_{CH_3}Cl and n'. Both k_f and k_s describe barrier-free ion−molecule reactions and are found to be very close to the capture limited rate coefficient, as discussed below. With this the unimolecular dissociation rate k_Γ becomes experimentally accessible, the inverse of which is the lifetime of the excited collision complex [$Cl^- \cdots CH_3Cl$]*.

The experimental setup[57] is based on a 22-pole trap as the reaction chamber for Cl$^-$ anions. Neutral reactant gas CH$_3$Cl (purity 99.8%) and stabilizing agents (CH$_3$ Cl, He, or N$_2$) are applied at a well defined and well controllable density and temperature. The radiofrequency ion trap is shown in the inset of Figure 2 (housing omitted for clarity). Ion storage is achieved by 22 stainless steel rods (1 mm diameter) forming a 40 mm long cylindrical cage (inscribed diameter $2r_0$ = 10 mm). The

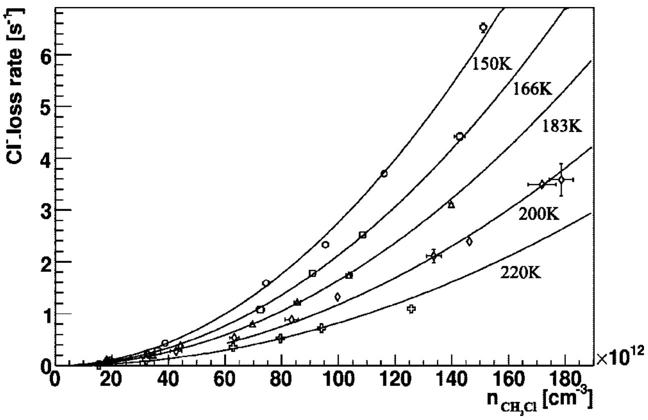

Figure 3. Cl^- loss rate due to the production of $[Cl^- \cdots CH_3Cl]$ as a function of the density of CH_3Cl buffer gas in the ion trap. The solid line shows a purely quadratic fit to the density dependence, yielding the three-body rate coefficient for the association and stabilization in collisions with CH_3Cl.

rods are alternatingly connected to the two opposite phase ports of a home-built rf oscillator[58] ($\omega/(2\pi) = 8.0$ MHz). While the ions are trapped in the radial direction by the cylindrical effective potential formed by the rf field, they are confined along the axis by small dc voltages (3−10 V) applied to cylindrical entrance and exit electrodes. The trap and its housing are mounted on a closed-cycle helium refrigerator and by this means its wall temperature, which determines the buffer gas temperature, is variable from 8−300 K. We measure the density of the CH_3 Cl reactant gas applied to the Cl^- anions in the trap by a gas-type-independent capacitance pressure gauge (Pfeiffer CMR 275) directly connected to the trapping volume. The different density inside the cryogenic trap compared to the pressure gauge due to thermal transpiration is calculated using the species-independent Knudsen value $[T_{gauge}/T_{trap}]^{1/2}$, which represents a very good approximation for the low densities employed in the trap.[59]

Ions are produced in an adjacent vacuum chamber and injected into the trap along its axis.[57] Cl^- anions are obtained from CCl_4 via dissociative attachment of slow electrons.[60] The ion source[61] employs a pulsed supersonic expansion of argon with a small admixture of CCl_4 bombarded by a pulsed 1 keV electron beam. In the created local plasma negative ions are formed and transferred to the trap with a Wiley−McLaren time-of-flight mass spectrometer.[62] Typically 2×10^3 Cl^- anions are trapped per filling. After extraction the ions are mass analyzed in a second time-of-flight stage before being detected on a microchannel plate. The time-of-flight mass spectra obtained after variable storage times show an exponential decay of the Cl^- ion signal as a function of storage time, as shown in Figure 2, and the corresponding formation of associated cluster ions with higher masses.[63]

3. Results and Discussion

The measured Cl^- decay rate in pure methyl chloride buffer gas is shown in Figure 3 as function of the methyl chloride density at different temperatures. It is found to be well fitted by the quadratic dependence $k_3 n^2_{CH_3Cl}$, which demonstrates the expected three-body association of stable $[Cl^- \cdots CH_3Cl]$ complexes according to eq 4. At 150 K a three-body rate coefficient of $(2.76 \pm 0.03) \times 10^{-28}$ cm^6/s is obtained from the fit. At lower temperatures the partial pressure of CH_3Cl reaches its vapor pressure and the buffer gas freezes to the trap walls. We observe the quadratic dependence for temperatures up to 220 K. At higher temperatures than 220 K an additional linear contribution to the Cl^- decay rate is observed, which dominates over the three-body association above 280 K.[64] In this study we therefore provide data on the temperature range between 150 and 220 K.

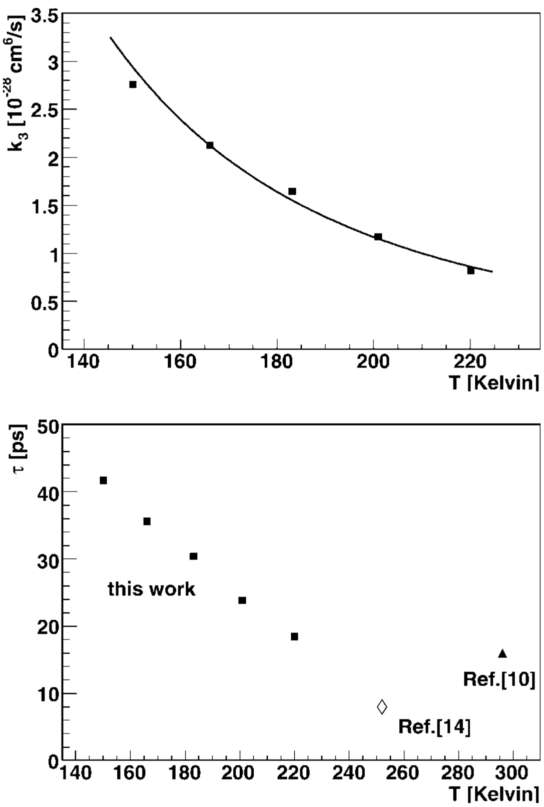

Figure 4. Upper panel: Measured ternary rate coefficient as a function of temperature; the symbol size indicates the accuracy, determined as fit error in Figure 3. A strong inverse temperature dependence is found, described by the fit $k_3 \propto T^{-n}$ with $n = 3.2 \pm 0.2$. Lower panel: Average lifetime of the S_N2 complex as a function of temperature. Our values (■), extracted from the ternary rate coefficients using bimolecular rate coefficients for association and stabilization, show a clear increase from 18 to 42 ps with decreasing temperature. In addition, the experimental value derived from high-pressure mass spectrometry at 296 K (▲)[10,28] and the result from a molecular dynamics calculation are shown (◇).[14,20]

In the upper panel of Figure 4 the measured three-body rate coefficient $k_3(T)$ is shown as a function of temperature. The symbol size represents the accuracy, determined as fit error in Figure 3. The three-body rate coefficient is found to show a strong inverse temperature dependence within the studied temperature range. The graph is reasonably well parametrized by the scaling law $k_3 \propto T^{-n}$, where the best fit of n yields 3.2 ± 0.2 (see Figure 4). We compare this exponent to the prediction of a statistical theory based on the principle of detailed balance.[34] This model suggests that $n = (r + 1)/2$, where r is the total number of rotational degrees of freedom of the separated association partners; excitation of the vibrational degrees of freedom of CH_3Cl does not play a role at the given temperatures. In our case of $[Cl^- \cdots CH_3Cl]$ association, the statistical model predicts $n = 1.5$, a temperature dependence much weaker than our experimental finding. Such a strong deviation from the statistical model is unusual for ternary association reactions.[38] This deviation shows that more thorough quantum mechanical methods may be needed. Also the low-energy vibrational modes of the complex may have to be included. This finding may also represent an indication for intrinsic nonstatistical dynamics in this S_N2 complex.

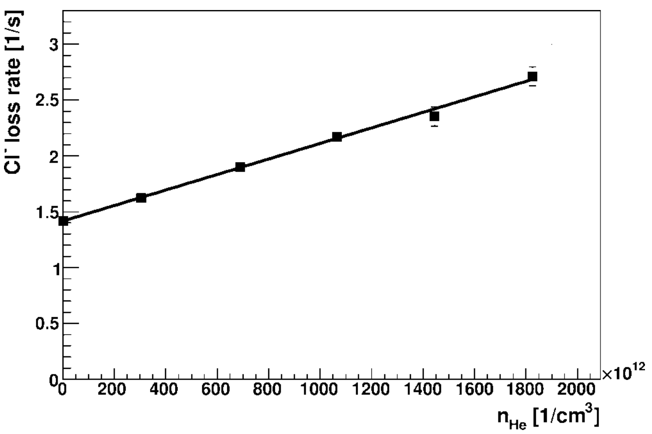

Figure 5. Cl^- loss rate due to production of $[Cl^- \cdots CH_3Cl]$ as a function of the density of He buffer gas when CH_3Cl is provided at constant density. From the slope of the linear density dependence the ratio of the stabilization efficiency β for different collision partners is derived (see text).

According to eq 4, the lifetime of the excited ion-dipole collision complex $[Cl^- \cdots CH_3Cl]^*$ can be derived from the ternary rate coefficient k_3 once the bimolecular rate coefficients for formation k_f and stabilization k_s for collisions with CH_3Cl are known. In previous studies of three-body association both these rate coefficients are usually assumed to be capture limited. We instead base our analysis on the association rate coefficients k_f derived from dedicated molecular dynamics trajectory simulations for reaction (2) (Table 6 of ref 14). These deviate slightly from capture theory calculations and are expected to map out the temperature dependence more accurately, which is important in this analysis. The stabilization rate k_s may be smaller than the capture limited rate due to inefficient energy transfer from the cluster vibrations to the collision partner. This is accounted for by parametrizing the stabilization rate as $k_s = \beta k_{\text{collision}}$, where $k_{\text{collision}}$ represents the capture rate and β denotes the probability for carrying away enough internal energy from the complex in a collision to prevent its dissociation. For the polar stabilizing agent CH_3 Cl the capture rate is obtained from the parametrization of classical trajectory results by Su and Chesnavich.[65,66] For the other employed stabilizing agents without a permanent dipole moment the temperature-independent Langevin collision rate is used.

In order to obtain information on the stabilization efficiency β, we experimentally compare the stabilization rates of different neutral collision partners. Figure 5 shows the conversion rate of Cl^- in the trap as a function of an applied helium density at 150 K while a constant density of CH_3Cl is maintained. For vanishing helium density the decay rate represents the three-body association with CH_3Cl as described above. Adding helium to the CH_3Cl buffer gas results in an additional contribution to the Cl^- conversion rate proportional to $n' = n_{He}$ (see eq 4). This linear dependence is reproduced in the data presented in Figure 5. By comparing this measurement, a similar measurement for nitrogen buffer gas, and the results for CH_3Cl, we derive ratios $\beta^{CH_3Cl}/\beta^{He} = (6.4 \pm 0.3)$ and $\beta^{CH_3Cl}/\beta^{N_2} = (1.15 \pm 0.04)$ at a temperature of 150 K. The two ratios reflect that for a larger intermediate three-body complex with an increased density of internal states, the transfer of at least part of the internal excitation of about 0.45 eV from the initial ion-dipole collision complex to the third body becomes more and more efficient. Most relevant for this energy transfer leading to stabilization are the low-energy cluster vibrations in the intermediate three-body complex. These vibrational modes correlate to translational and rotational motion of the separated collision partners. Interestingly, the ratio of β for N_2 and CH_3Cl is surprisingly close to unity. This implies that the stabilization efficiency saturates with respect to increasing the density of states in the three-body complex. Since the stabilization efficiency is expected to saturate when every collision leads to stabilization, we conclude that the rate coefficient for stabilization of the excited ion dipole complex with CH_3Cl is very close to the collision limit and thus $\beta^{CH_3Cl} \approx 1$. Support for this conclusion stems from the fact that the formation of excited $[Cl^- \cdots CH_3Cl]^*$ complexes proceeds via translational to rotational ($T \rightarrow R$) energy transfer[4] so that stabilization with a second CH_3Cl molecule can occur via $R \rightarrow R$ and $R \rightarrow T$ transfer, both of which are likely to be very efficient. Based on this description we assume β lies near unity for CH_3Cl also for temperatures higher than 150 K.

Using eq 4 and the association and stabilization rate coefficients as described above, lifetimes $\tau = k_\Gamma^{-1}$ of the ion-dipole complex $[Cl^- \cdots CH_3Cl]^*$ are derived from the temperature-dependent three-body rate coefficient $k_3(T)$. The results are shown in the lower panel of Figure 4 as a function of the association temperature. Again, the symbol size represents the statistical experimental accuracy. At the lowest studied temperature of 150 K, we determine a lifetime of 42 ps. The lifetime then decreases with increasing temperature reaching a value of 18 ps at 220 K. This decrease in lifetime for higher temperature is an experimental indication for the corresponding increase of the density of states for the loose transition state corresponding to the Cl^- and CH_3Cl reactants.

Our measured lifetimes are shown in the lower panel of Figure 4 together with a theoretical value, which stems from trajectory calculations. It has been obtained for an excess energy corresponding to 250 K and for a rotational temperature of 300 K of the CH_3Cl reactant.[14,20] The theoretical value suggests a continuation of the linear temperature dependence of the $[Cl^- \cdots CH_3Cl]^*$ complex to 250 Kelvin. On the other hand the previous room temperature measurement by high-pressure mass spectrometry[10,28] is quite similar to our value measured at 220 K, as seen from Figure 4. This suggests that the strong temperature dependence observed below 220 K changes to a much weaker dependence for higher temperatures.

The femtosecond pump–probe measurement of $[I^- \cdots CH_3I]^*$[11] as well as the classical trajectory calculations[14,20] yield multiexponential decay curves of metastable S_N2 complexes. It should be noted that the present experiment as well as the previous high-pressure mass spectrometry study at room temperature[10,28] are only sensitive to average complex lifetimes.

Longer average lifetimes of the entrance channel complex at lower temperatures give S_N2 reaction systems more time to exploit the available phase space, randomize energy, and finally cross the barrier and form reaction products. Therefore enhanced metastable lifetimes are likely to cause the strong inverse temperature dependence observed in the rate to form reaction products in nonsymmetric S_N2 reactions.[27] In addition, at low temperature S_N2 reaction dynamics may even change from nonstatistical to statistical due to the longer available time for intramolecular energy redistribution.

4. Conclusion

In this study we present experimental evidence for a strong inverse temperature dependence of the average lifetime of transient S_N2 ion-dipole complexes. These data are obtained by analyzing three-body association of $[Cl^- \cdots CH_3Cl]^*$ in a low-temperature ion trap. A temperature dependence of the ternary association rate coefficient is found that is in disagreement with the prediction of a simple statistical model. This shows that this S_N2 system may need more advanced quantum mechanical methods to explain the observed temperature dependence. In measurements with different collision partners the stabilization efficiency for ternary collisions with CH_3 Cl is found to be capture limited. With this information it became possible to extract the average lifetimes of metastable $[Cl^- \cdots CH_3Cl]^*$ from the ternary rate coefficients in the temperature range from 150 to 220 K. In the future, we will improve the experimental setup to extend the lifetime measurements to a larger temperature range. This will allow us to track the break-off suggested by the room-temperature lifetime.[10,28]

The temperature dependence of the lifetime observed in this work suggests that the inverse temperature dependence of reaction rate coefficients for nonsymmetric nucleophilic substitution reactions may also be traced back to temperature-dependent lifetimes of the transient entrance channel complex. Furthermore, the observed lifetimes suggest that statistical dynamics may be favored over nonstatistical dynamics at very low temperatures. For the future, the low-temperature ion trap provides an ideal tool to study the reaction of isotopically labeled symmetric S_N2 reactions. This will allow one to clarify the role of tunneling through and recrossings over the intermediate potential barrier.

Acknowledgment. We thank Al Viggiano and Bill Hase for stimulating discussions and their comments on the manuscript. This work is supported by the Eliteförderprogramm der Landesstiftung Baden-Württemberg and by the Deutsche Forschungsgemeinschaft.

References and Notes

(1) Chabinyc, M. L.; Craig, S. L.; Regan, C. K.; Brauman, J. I. *Science* **1998**, *279*, 1882.

(2) Regan, C. K.; Craig, S. L.; Brauman, J. I. *Science* **2002**, *295*, 2245.

(3) Laehdahl, J. K.; Uggeruk, E. *Int. J. Mass Spectrom.* **2002**, *214*, 277.

(4) Hase, W. L. *Science* **1994**, *266*, 998.

(5) Sun, L.; Song, K.; Hase, W. L. *Science* **2002**, *296*, 875.

(6) Schmatz, S. *ChemPhysChem* **2004**, *5*, 600.

(7) Mikosch, J.; Trippel, S.; Eichhorn, C.; Otto, R.; Lourderaj, U.; Zhang, J. X.; Hase, W. L.; Weidemüller, M.; Wester, R. *Science* **2008**, *319*, 183.

(8) Craig, S. L.; Brauman, J. I. *Science* **1997**, *276*, 1536.

(9) Craig, S. L.; Zhong, M.; Brauman, J. I. *J. Am. Chem. Soc.* **1999**, *121*, 11790.

(10) Li, C.; Ross, P.; Szulejko, J. E.; McMahon, T. B. *J. Am. Chem. Soc.* **1996**, *118*, 9360.

(11) Wester, R.; Bragg, A. E.; Davis, A. V.; Neumark, D. M. *J. Chem. Phys.* **2003**, *119*, 10032.

(12) Olmstead, W. N.; Brauman, J. I. *J. Am. Chem. Soc.* **1977**, *99*, 4219.

(13) DePuy, C. H.; Gronert, S.; Mullin, A.; Bierbaum, V. M. *J. Am. Chem. Soc.* **1990**, *112*, 8650.

(14) Linde, S. R. V.; Hase, W. L. *J. Chem. Phys.* **1990**, *93*, 7962.

(15) Linde, S. R. V.; Hase, W. L. *J. Phys. Chem.* **1990**, *94*, 6148.

(16) Viggiano, A. A.; Morris, R. A.; Paschkewitz, J. S.; Paulson, J. F. *J. Am. Chem. Soc.* **1992**, *114*, 10477.

(17) Graul, S. T.; Bowers, M. T. *J. Am. Chem. Soc.* **1990**, *113*, 9696.

(18) Graul, S. T.; Bowers, M. T. *J. Am. Chem. Soc.* **1994**, *116*, 3875.

(19) Graul, S. T.; Carpenter, C. J.; Bushnell, J. E.; van Koppen, P. A. M.; Bowers, M. T. *J. Am. Chem. Soc.* **1998**, *120*, 6785.

(20) Peslherbe, G. H.; Wang, H.; Hase, W. L. *J. Chem. Phys.* **1995**, *102*, 5626.

(21) Clary, D. C.; Palma, J. *J. Chem. Phys.* **1997**, *106*, 575.

(22) Schmatz, S.; Botschwina, P.; Hauschildt, J.; Schinke, R. *J. Chem. Phys.* **2001**, *114*, 5233.

(23) Hennig, C.; Schmatz, S. *J. Chem. Phys.* **2005**, *122*, 234307.

(24) Hauschildt, J.; Schinke, R.; Schmatz, S.; Botschwina, P. *Phys. Chem. Chem. Phys.* **2001**, *3*, 2275.

(25) Hennig, C.; Schmatz, S. *J. Chem. Phys.* **2004**, *121*, 220.

(26) Schmatz, S.; Hauschildt, J. *J. Chem. Phys.* **2003**, *118*, 4499.

(27) Le Garrec, J. L.; Rowe, B. R.; Queffelec, J. L.; Mitchell, J. B. A.; Clary, D. C. *J. Chem. Phys.* **1997**, *107*, 1021.

(28) Note the corrected value of 16 ps as compared to 27 ps in the publication; the authors may have misinterpreted the units of the values in table VI of ref 14 which they used in their data analysis.

(29) Adams, N. G.; Smith, D. *Chem. Phys. Lett.* **1981**, *79*, 563.

(30) Adams, N. G.; Smith, D. *Int. J. Mass Spectrom. Ion Processes* **1987**, *81*, 273.

(31) Glosík, J.; Zakouřil, P.; Lindinger, W. *Int. J. Mass Spectrom. Ion Processes* **1995**, *145*, 155.

(32) Smith, M. A. *Int. Rev. Phys. Chem.* **1998**, *17*, 35.

(33) Schlemmer, S.; Luca, A.; Glosík, J.; Gerlich, D. *J. Chem. Phys.* **2002**, *116*, 4508.

(34) Herbst, E. *J. Chem. Phys.* **1979**, *70*, 2201.

(35) Herbst, E. *Chem. Phys.* **1982**, *68*, 323.

(36) Bates, D. R. *J. Phys. B* **1979**, *12*, 4135.

(37) Bass, L. M.; Jennings, K. R. *Int. J. Mass Spectrom. Ion Processes* **1984**, *58*, 307.

(38) Viggiano, A. A. *J. Chem. Phys.* **1986**, *84*, 244.

(39) Linde, S. R. V.; Hase, W. L. *J. Phys. Chem.* **1990**, *94*, 2778.

(40) DeTuri, V. F.; Hintz, P. A.; Ervin, K. M. *J. Phys. Chem. A* **2001**, *101*, 5969.

(41) Dougherty, R. C.; Dalton, J.; Roberts, J. D. *Org. Mass Spectrom.* **1977**, *8*, 77.

(42) Larson, J. W.; McMahon, T. B. *J. Am. Chem. Soc.* **1984**, *106*, 517.

(43) Larson, J. W.; McMahon, T. B. *J. Am. Chem. Soc.* **1985**, *107*, 766.

(44) Barlow, S. E.; Doren, J. M. V.; Bierbaum, V. M. *J. Am. Chem. Soc.* **1988**, *110*, 7240.

(45) Gerlich, D. *Phys. Scr.* **1995**, *T59*, 256.

(46) Trippel, S.; Mikosch, J.; Berhane, R.; Otto, R.; Weidemüller, M.; Wester, R. *Phys. Rev. Lett.* **2006**, *97*, 193003.

(47) Mikosch, J.; Frühling, U.; Trippel, S.; Schwalm, D.; Weidemüller, M.; Wester, R. *Phys. Rev. Lett.* **2007**, *98*, 223001.

(48) Paul, W.; Lücke, B.; Schlemmer, S.; Gerlich, D. *Int. J. Mass Spectrom. Ion Processes* **1995**, *149* (150), 373.

(49) Paul, W.; Schlemmer, S.; Lücke, B.; Gerlich, D. *Chem. Phys.* **1996**, *209*, 265.

(50) Gerlich, D.; Horning, S. *Chem. Rev.* **1992**, *92*, 1509.

(51) Asvany, O.; Kumar, P.; Redlich, B.; Hegemann, I.; Schlemmer, S.; Marx, D. *Science* **2005**, *309*, 1219.

(52) Dzhonson, A.; Jochnowitz, E. B.; Maier, J. P. *J. Phys. Chem. A* **2007**, *111*, 1887.

(53) Otto, R.; Mikosch, J.; Trippel, S.; Weidemüller, M.; Wester, R. *Phys. Rev. Lett.* **2008**, *101*, 063201.

(54) Glosík, J.; Hlavenka, P.; Plašil, R.; Windisch, F.; Gerlich, D.; Wolf, A.; Kreckel, H. *Phil. Trans. R. Soc. A* **2006**, *364*, 2931.

(55) Stearns, J. A.; Mercier, S.; Seaiby, C.; Guidi, M.; Boyarkin, O. V.; Rizzo, T. R. *J. Am. Chem. Soc.* **2007**, *129*, 11814.

(56) Mikosch, J.; Kreckel, H.; Wester, R.; Plasil, R.; Glosik, J.; Gerlich, D.; Schwalm, D.; Wolf, A. *J. Chem. Phys.* **2004**, *121*, 11030.

(57) Mikosch, J.; Frühling, U.; Trippel, S.; Otto, R.; Hlavenka, P.; Schwalm, D.; Weidemüller, M.; Wester, R. *Phys. Rev. A* **2008**, *78*, 023402.

(58) Jones, R.; Anderson, S. *Rev. Sci. Instrum.* **2000**, *71*, 4335.

(59) Jitschin, W.; Röhl, P. *J. Vac. Sci. Technol. A* **1987**, *5*, 372.

(60) Matejčík, S.; Foltin, V.; Stano, M.; Skalný, J. D. *Int. J. Mass Spectrom.* **2002**, *223*, 9.

(61) Alexander, M.; Levinger, N. E.; Johnson, M. A.; Ray, D.; Lineberger, W. C. *J. Chem. Phys.* **1988**, *88*, 6200.

(62) Wiley, W. C.; McLaren, I. H. *Rev. Sci. Instrum.* **1955**, *26*, 1150.

(63) Due to HCl impurities in the CH_3Cl buffer gas, the formed $[Cl^- \cdots CH_3Cl]$ complex is an intermediate species that converts to the much deeper bound hydrogen bonded bihalide $ClHCl^-$ cluster[67] by subsequent ligand switching with HCl. Further coagulation followed by collisional dissociation make the mass spectra difficult to interpret in detail. Nevertheless the three-body association $Cl^- + CH_3Cl \rightarrow [Cl^- \cdots CH_3Cl]$ is identified as the rate determining step, the rate of which is given by the measured Cl^- decay rate according to eq 4.

(64) We attribute the linearly density-dependent loss process that is observed for temperatures higher than 220 K to a combination of collision induced dissociation and bimolecular reactions with buffer gas impurities.

(65) Su, T.; Chesnavich, W. J. *J. Chem. Phys.* **1982**, *76*, 5183.

(66) Su, T. *J. Chem. Phys.* **1988**, *89*, 5355.

(67) Caldwell, G.; Kebarle, P. *Can. J. Chem.* **1985**, *63*, 1399.

JP804655K